PIS-Net: A Novel Pixel Interval Sampling Network for Dense Microorganism Counting in Microscopic Images

Jiawei Zhang[1], Chen Li[1(✉)], Hongzan Sun[2], and Marcin Grzegorzek[3]

[1] Microscopic Image and Medical Image Analysis Group, College of Medicine and Biological Information Engineering, Northeastern University, Shenyang, China
1971087@stu.neu.edu.cn, lichen@bmie.neu.edu.cn
[2] Shengjing Hospital, China Medical University, Shenyang, China
sunhz@sj-hospital.org
[3] Institute for Medical Informatics, University of Luebeck, Lübeck, Germany
marcin.grzegorzek@uni-luebeck.de

Abstract. A novel Pixel Interval Sampling Network (PIS-Net) is applied here for dense microorganism counting. The PIS-Net is designed for microorganism image segmentation with encoder to decoder architecture, and then the connected domain detection is applied for counting. The proposed method has good response for edge segmentation between tiny objects. Several classical segmentation metrics (Dice, Jaccard, and Hausdorff distance) are applied for evaluation. Experimental result shows that the proposed PIS-Net has the best performance and potential for dense tiny object counting tasks, which achieves 96.88% counting accuracy on the dataset with 420 yeast cell images. By comparing with the state-of-the-art approaches like Attention U-Net, Swin U-Net, and Trans U-Net, the proposed PIS-Net can segment the dense tiny objects with clearer boundaries and fewer incorrect debris, which shows the great potential of PIS-Net in the task of accurate counting tasks.

Keywords: Microorganism counting · Pixel interval sampling · Image segmentation · Deep learning · Dense objects

1 Introduction

The problem of environmental pollution needs to be resolved with the development of urbanization. With the break of Corona Virus Disease 2019 (COVID-19), people pay more attention to the microorganism analysis [20,22]. The biological methods, which are more efficient with no pollution, are widely applied for pollution controlling by comparing with physical and chemical methods. Yeast is a kind of single-celled eukaryotic microorganism, which was first applied in wastewater treatment and performed startlingly [29], and it can also be applied for the treatment of toxic industrial wastewater and solid waste [34] till now.

E. Pietka et al. (Eds.): ITIB 2022, AISC 1429, pp. 307–318, 2022.
https://doi.org/10.1007/978-3-031-09135-3_26

The research of yeast counting can quantitatively evaluate the performance of yeast in various tasks [30]. The classical counting methods are stable and straightforward, but they are subjective, and the counting accuracy is unsatisfactory when the number of cells becomes larger. With the development of digital image processing and machine learning technologies, image analysis-based approaches are widely applied for microorganism classification, segmentation, and counting [16–19,26,35,36,38]. However, by reviewing our recent work [14], we find that deep learning methods are mostly applied for microorganism classification, but not for microorganism segmentation in the task of microorganism counting. To improve the performance of dense tiny microorganism counting, we propose a novel *Pixel Interval Sampling Network* (PIS-Net) for the yeast counting task with higher accuracy. The PIS-Net is designed as an Encoder-Decoder architecture based on Convolutional Neural Network (CNN), pixel interval sampling, and concatenate operations. The proposed PIS-Net has improved counting performance by comparing with SegNet [3] and U-Net [23]. The workflow of the proposed PIS-Net counting method is shown in Fig. 1.

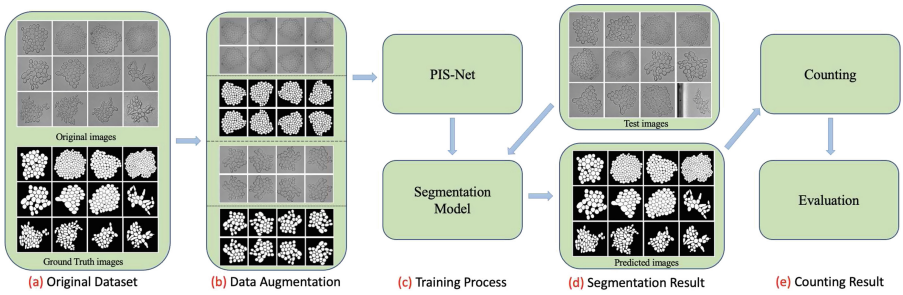

Fig. 1. The workflow of PIS-Net-based dense tiny microorganism counting system

In Fig. 1, (a) Original Dataset: The dataset contains images of yeast cells and their ground truth (GT). There are less than 256 yeast cells in each image. (b) Data Augmentation: Mirror and rotation operations are applied to expand the original dataset. (c) Training Process: PIS-Net is trained for image segmentation, and the model with the best performance is saved. (d) Segmentation Result: Using the best PIS-Net model to output the segmentation binary images. (e) Counting Result: The number of yeast cells is counted by using connected domain detection.

The main contributions of this paper are as follows: (1) We propose the PIS-Net for dense tiny object counting. All down-sampling operations are based on pixel interval sampling without max-pooling. (2) The operation of max-pooling would lose some local features of tiny objects (the edge lines may not be connected after max-pooling operations), while PIS-Net can cover a more detailed region. (3) The proposed PIS-Net achieves the best counting result by comparing it with other models.

2 Related Work

In Table 1, the digital image processing-based microorganism counting approaches are listed, including classical and machine learning-based counting approaches. Our survey paper [14] summarized and analyzed these methods in detail.

Table 1. Microorganism image counting methods

Category	Subcategory	Related work
Classical methods	Thresholding based methods	[2,10,33]
	Edge detection based methods	[4,5,27]
	Watershed based methods	[1,13,24]
Machine learning	Classical machine learning based methods	[28,37]
Methods	Deep learning based methods	[6,12]

Classical Counting Methods. The segmentation result determines the performance of microorganism counting. In Table 1, the classical approaches are listed, which contain thresholding, edge detection, and watershed based methods. Many kinds of thresholding approaches are applied for microorganism counting tasks [2,10,33]. In [2], the iterative local threshold is applied for bacteria image segmentation, and then a Hough circle transformation is used to separate clustered colonies into a single colony. In [10], an adaptive thresholding method is applied for image segmentation, then, the minima function is used for center locating of the microorganism. The work [33] uses Otsu thresholding for bacteria image segmentation, and the hypothesis testing is then used for debris erasing. Edge detection approaches are applied for microorganism image counting [4,5,27]. In [4], several combination approaches of different edge detection filters are applied for the microorganism counting tasks. Then the concave surface between the connected colonies is detected for counting. In [27], Sobel and Laplacian filters are applied for bacteria edge detection. In [1,13,24], watershed approaches are applied for microorganism counting. In [1], a watershed-based method is used for bacteria images colonies separation. Then, the circularity ratio of colonies is measured and counted. In [13], distance transformation is combined with watershed and applied for the bacteria counting task. Then, the sharp corners are eliminated by using morphological operations.

Machine Learning-Based Counting Methods. In Table 1, the counting methods based on classical machine learning and deep learning are summarized. In [28], Principal Component Analysis (PCA) is used to separate the bacteria with useless debris. Then, the nearest neighbor searching technology is used to separate the clustered colonies. In [37], Support Vector Machine (SVM) is

trained using shape features for different microorganisms classification, then the Otsu thresholding is used for counting. In [6], the Marr-Hildreth operator is used to detect the edge of bacteria images. Then thresholding is used for binary image segmentation. After that, Artificial Neural Network (ANN) is trained for bacteria classification. In [12], the contrast-limited adaptive histogram equalization is used to segment the bacteria. Moreover, a neural network including four convolutional and one fully connected layers is used for microorganism image classification. By analyzing all related works, it can be found that in the task of microorganism counting, most deep learning approaches are used for classification tasks, but few for segmentation tasks. The classical segmentation approaches perform unsatisfactorily through the pre-test because the contour lines of yeast cells in our dataset are not clear. So we design an end-to-end CNN model for the tasks of dense tiny objects segmentation.

3 PIS-Net-Based Yeast Counting Method

3.1 Image Dataset

In our work, we use a yeast image dataset proposed in [11], containing 51 different images of yeast cells and their corresponding ground truth (GT) images. The images contain 3799 yeast cells in total. All images are resized to the resolution of 256×256 pixels, which are shown in Fig. 2. Then the original 51 images are rotated (0, 90, 180, and 270°C) and flipped (mirror), so the number of images in this dataset is augmented to eight times (408 images).

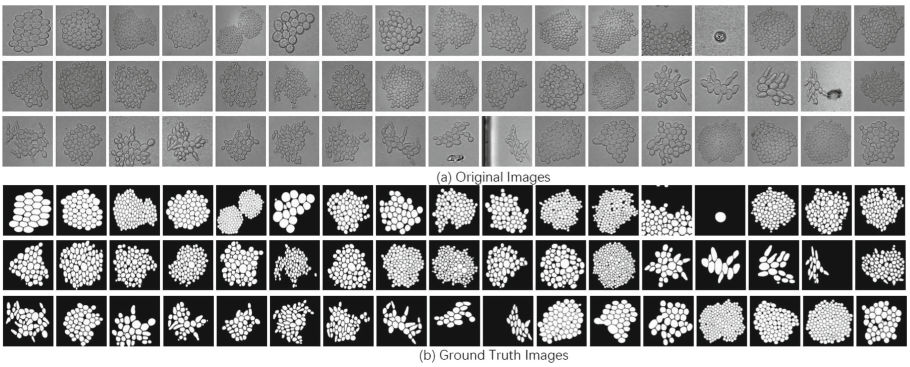

Fig. 2. The images in yeast cell dataset (a) shows the original yeast image and (b) is the corresponding Ground Truth images

The augmented yeast image dataset is randomly divided into training, validation, and test dataset with the ratio of 3:1:1. Therefore, 244 original and their corresponding GT images are used for the training task, 82 original and their corresponding GT images are used for validation, and 82 original images are used for the test.

3.2 The Structure of PIS-Net

The structure of the proposed PIS-Net is shown in Fig. 3, which is an end-to-end CNN structure based on the encoder and decoder. There are four blocks in the encoder network (red dotted box in Fig. 3). The first part in each block are two convolution operations with a kernel size of 3×3 (each use filtering with padding and followed by a ReLU operation), then the pixel interval sampling operation is applied to reduce the size of feature maps by half. The architecture of pixel interval sampling is shown in Fig. 3. It shows that the feature maps with channel C can be processed into 4 parts based on pixel interval sampling, and they then can be combined using concatenation operations. To further extract features of feature maps, while considering the finite computational ability, convolution operations with the kernel size of 3×3 (filtering with padding and activated with ReLU) can tune 4 C-dimensional features to C-dimensional features. Hereto, the initial feature maps with size $H \times W$ and channel C are changed to feature maps with size $\frac{H}{2} \times \frac{W}{2}$ and channel C. The procedure is repeated four times, with output resolutions of $\frac{H}{16} \times \frac{W}{16}$ and channel of $4C$.

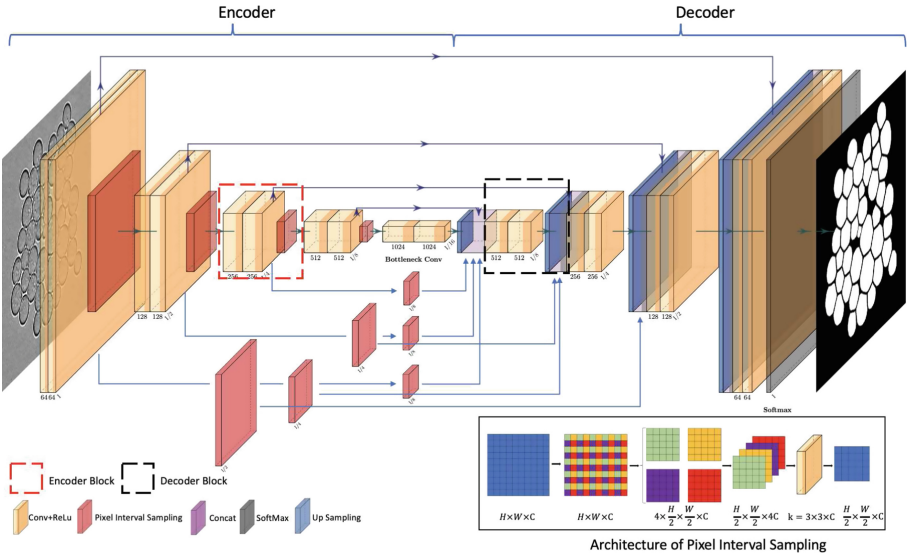

Fig. 3. The network structure of PIS-Net

In decoder network, four blocks are applied for up-sampling. Two convolution operations with a kernel size of 3×3 (each use filtering with padding and followed by a ReLU operation) are applied first. Then the transposed convolution operation with a kernel size of 3, a stride of 2, and padding of 1 is applied for up-sampling. The transposed convolution, whose parameters can be learned in the process of backpropagation, can be applied to expand the size of the

image [32]. Meanwhile, the number of channels can be changed by using the different number of convolutional kernels [31]. After that, the high-resolution feature maps from the encoder are transformed to low-resolution feature maps using 2×, 4× and 8× pixel interval sampling, and concatenated with the feature maps after up-sampling. For instance, the 8× pixel interval sampling features of the first block, 4× pixel interval sampling of the second block and 2× pixel interval sampling of the third block in the encoder are concatenated with the copied features of the fourth block and the features after up-sampling (5 parts of pixel interval sampling features are concatenated in the fourth level of the decoder). In the same way, there are 4, 3, 2 parts of features are concatenated in the third, second, and first level of decoder, respectively. After that, two convolutions and ReLU operations are applied to change the number of channels. The up-sampling operation is repeated four times, with output resolutions of $H \times W$ and channel of C, which has the same size as the encoder input features. Finally, a Softmax layer with 2 output channels is applied for feature maps classification.

3.3 Counting Method

After segmentation, the post-processing method is applied to reduce the effect of noises. A morphological filter is applied to remove small regions, which can significantly improve the counting performance. Finally, the connected regions of the segmentation images after post-processing are counted based on 8 Neighborhood Search [7].

4 Experiments

4.1 Experimental Setting

Evaluation Indices. The evaluation indices are listed in Table 2. TP (True Positive), TN (True Negative), FP (False Positive), and FN (False Negative) are basic evaluation metrics, which can be applied to measure the performance of segmentation in general. Furthermore, N_{pred} means the number of connected regions in the predicted image, N_{GT} means the number of connected regions in the GT image, which indicates the number of yeast cells. In the definition of Hausdorff distance, sup is supremum and inf is infimum. Hausdorff distance can be applied to measure the shortest distance between two images, with the unit of pixels per image.

Experimental Environment. The experiment is conducted by Python 3.8.10 in Windows 10 operating system. The experimental environment is based on Torch 1.9.0. The workstation is equipped with Intel(R) Core(TM) i7-8700 CPU with 3.20 GHz, 16 GB RAM, and NVIDIA GEFORCE RTX 2080 8 GB.

Table 2. The definitions of evaluation metrics. CA and HD are abbreviations of counting accuracy and hausdorff distance, respectively

Metric	Definition
Accuracy	$\frac{TP+TN}{TP+TN+FP+FN}$
Jaccard	$\frac{TP+TN}{FN+TP+FP}$
Dice	$\frac{2TP}{FN+2TP+FP}$
Precision	$\frac{TP}{TP+FP}$
CA	$1-\frac{\lvert N_{pred}-N_{GT}\rvert}{N_{GT}}$
HD	$d_H(X,Y)=\max(\sup_{x\in X}\inf_{y\in Y}d(x,y),\sup_{y\in Y}\inf_{x\in X}d(x,y))$

Parameters Setting. Softmax is used for the final classification in our experiment. Adam optimizer is applied to minimize the loss function, which can adjust the learning rate automatically by considering the gradient momentum of the previous time steps [15]. In the training task, the learning rate is set as 0.001, and the batch size is 8. The epoch is set as 100 by considering the converging speed of experimental models, the example of loss and intersection over union (IoU) curves of models is shown in Fig. 4. Though there are 92,319,298 params to be trained in total, the PIS-Net can converge rapidly and smoothly, without overfitting. There is a jump in loss and IoU plots for all 3 tested networks from 40 to 80 epochs, which is caused by the small batch size. Small batch size may lead to the huge differences between each batch, and the loss and IoU curves may jump while convergence.

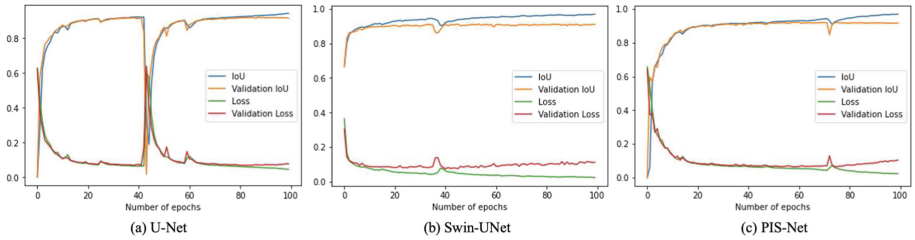

Fig. 4. The loss and IoU curves in training process

4.2 Evaluation of Segmentation and Counting Performance

To show the best performance of PIS-Net for the task of yeast counting, we compare it with some state-of-the-art methods, which contain Attention U-Net [21], Trans U-Net [9], and Swin U-Net [8].

The experimental setting and evaluation indices are the same for the comparative experiment. All comparative experiments have the same dataset for

training, validation, and test, which is proposed in Sect. 3.1. All models are trained from scratch without pre-training and fine-tuning, which are the same as the work in [11] (though the models after pre-trained may obtain more satisfactory results). In addition, the methods based on Hough transformation, Otsu thresholding, and Watershed are compared to show the performance of classical methods in the task of tiny dense object counting. The images after segmentation are shown in Fig. 5.

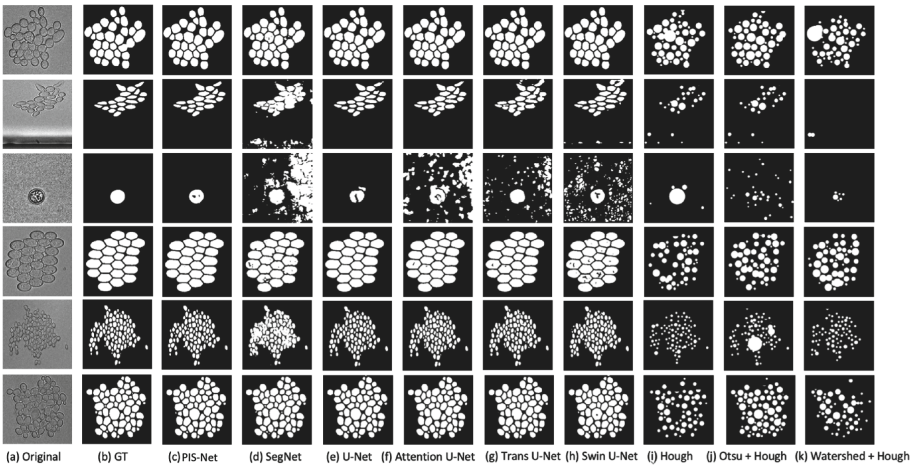

Fig. 5. An example of segmentation images predicted by different models

By reviewing the Table 3, it shows that the PIS-Net has the highest Dice, Jaccard, and Precision, which indicates that the PIS-Net performs best in the task of dense tiny objects segmentation. U-Net has better Accuracy and Hausdorff distance, but the values are close to the proposed PIS-Net. It can be seen that the deep learning methods can work better than the classical methods in this task.

After segmentation, post-processing proposed in Sect. 3.3 is applied for noise removal. Then the region search method based on 8 Neighborhood is applied for dense tiny object counting. The counting results of several methods are shown in Table 4.

The Counting accuracy of PIS-Net is the best and more than 5% higher than U-Net. The Counting Accuracy of SegNet, Attention-UNet, Trans U-Net, and Swin U-Net would be less than zero without post-processing, which is caused by the huge number of False Positive pixels.

4.3 Repeatability Tests

Five extra experiments are done for repeatability tests to prove the stable and accurate segmentation performance of PIS-Net. The result is shown in Table 5.

Table 3. The average segmentation evaluation indices of predicted images (accuracy, dice, jaccard and precision are in [%], hausdorff distance is in pixel per image)

Methods	Accuracy	Dice	Jaccard	Precision	Hausdorff distance
PIS-Net	97.42	**95.75**	**91.89**	**95.68**	4.72
SegNet	94.69	90.34	84.02	88.50	6.36
U-Net	**97.47**	95.71	91.84	95.62	**4.67**
Attention U-Net	96.62	93.36	88.96	92.67	5.12
Trans U-Net	96.84	93.60	88.99	93.25	5.07
Swin U-Net	96.47	92.99	88.32	92.43	5.31
Hough	82.12	61.12	44.74	88.26	9.25
Otsu	84.23	65.71	49.90	87.66	8.92
Watershed	78.67	50.15	34.88	78.61	9.69

Table 4. The average counting accuracy of predicted images (in %)

Methods	Counting accuracy	Methods	Counting accuracy
PIS-Net	**96.88**	SegNet	68.82
U-Net	91.33	Attention U-Net	84.34
Trans U-Net	91.32	Swin U-Net	91.95
Hough	73.66	Otsu	74.34
Watershed	63.34		

From Table 5, it can be found that all evaluation indices of repeated PIS-Nets are approximate, which shows satisfactory and stable counting performance for dense tiny object counting tasks.

Table 5. The evaluation indices of repeatability tests (accuracy, dice, jaccard, precision and counting accuracy are in %, hausdorff distance is in pixel per image)

Methods	Accuracy	Dice	Jaccard	Precision	Counting accuracy	Hausdorff distance
PIS-Net	97.42	95.75	91.89	95.68	96.88	4.72
PIS-Net (Re 1)	97.51	95.79	91.97	95.91	95.26	4.59
PIS-Net (Re 2)	97.33	95.59	91.62	95.70	96.25	4.73
PIS-Net (Re 3)	97.54	95.91	92.18	96.21	96.82	4.60
PIS-Net (Re 4)	97.37	95.64	91.70	95.70	95.51	4.75
PIS-Net (Re 5)	97.43	95.66	91.73	92.24	96.26	4.64

4.4 Computational Time

The training time, mean training time, test time, and mean test time are listed in Table 6. There are 244 images in the training dataset and 82 images in the test dataset. The mean training time of the PIS-Net model is approximately 1.8 s higher than the time of the Swin U-Net, and the test time is about 0.28 s higher than Swin U-Net. The memory cost of PIS-Net is about 36MB, which is about 6MB less than the cost of Swin U-Net model, meanwhile, the PIS-Net has better counting performance. The counting accuracy is increased by about 6%, so the PIS-Net has satisfactory counting performance and tolerable computational time, which can be widely applied in the task of accurate dense tiny object counting.

Table 6. The summary of computational time (in seconds)

Model	Training time	Mean training time	Test time	Mean test time
PIS-Net	1750.80	7.18	76.23	0.93
U-Net	1033.00	4.23	42.94	0.52
Swin-UNet	1314.06	5.39	53.25	0.65
Att-UNet	1163.93	4.77	49.44	0.60

5 Conclusion and Future Work

In this paper, a CNN model, PIS-Net is designed for the task of dense tiny objects (yeast) counting. PIS-Net is an end-to-end model based on the encoder to decoder architecture, down-sampling operations are based on pixel interval sampling without max-pooling, which can cover more detailed regions and decrease the accuracy loss of down-sampling in the task of dense tiny objects counting. The evaluation indices, including Accuracy, Dice, Jaccard, Precision, Counting Accuracy, and Hausdorff Distance of PIS-Net are 97.42%, 95.75%, 91.89%, 95.68%, 96.48% and 4.7204. By comparing with U-Net, the Dice, Jaccard, Precision, and Counting Accuracy are improved by 0.04%, 0.05%, 0.06%, 0.4% and 5.55%, respectively, which shows the PIS-Net has excellent segmentation and counting performance in the tasks of dense tiny objects counting. However, the Accuracy is decreased by 0.05% and Hausdorff Distance is improved by 0.0538, which shows there is still some room for improvement.

In the future, we plan to apply pixel interval sampling for down-sampling in other models to reduce the accuracy loss caused by max-pooling. On the other hand, we will improve the architecture of PIS-Net for better segmentation and counting performance. The model pruning [25] can also be applied to control the memory cost of PIS-Net, making it more stable to use.

Acknowledgement. This work is supported by "National Natural Science Foundation of China" (No. 61806047).

References

1. Ates, H., Gerek, O.: An image-processing based automated bacteria colony counter. In: Proceedings of ISCIS 2009, pp. 18–23 (2009)
2. Austerjost, J., Marquard, D., Raddatz, L., et al.: A smart device application for the automated determination of E. coli colonies on agar plates. Eng. Life Sci. **17**(8), 959–966 (2017)
3. Badrinarayanan, V., Kendall, A., Cipolla, R.: Segnet: a deep convolutional encoder-decoder architecture for image segmentation. IEEE Trans. Pattern Anal. Mach. Intell. **39**(12), 2481–2495 (2017)
4. Barbedo, J.: An algorithm for counting microorganisms in digital images. IEEE Lat. Am. Trans. **11**(6), 1353–1358 (2013)
5. Barber, P., Vojnovic, B., Kelly, J., et al.: An automated colony counter utilising a compact Hough transform. Proc. MIUA **2000**, 41–44 (2000)
6. Blackburn, N., Hagström, Å., Wikner, J., et al.: Rapid determination of bacterial abundance, biovolume, morphology, and growth by neural network-based image analysis. Appl. Environ. Microbiol. **64**(9), 3246–3255 (1998)
7. Boss, R., Thangavel, K., Daniel, D.: Automatic mammogram image breast region extraction and removal of pectoral muscle. arXiv: 1307.7474 (2013)
8. Cao, H., Wang, Y., Chen, J., et al.: Swin-unet: unet-like pure transformer for medical image segmentation. arXiv: 2105.05537 (2021)
9. Chen, J., Lu, Y., Yu, Q., et al.: Transunet: Transformers make strong encoders for medical image segmentation. arXiv: 2102.04306 (2021)
10. Clarke, M., Burton, R., Hill, A., et al.: Low-cost, high-throughput, automated counting of bacterial colonies. Cytometry Part A **77**(8), 790–797 (2010)
11. Dietler, N., Minder, M., Gligorovski, V., et al.: A convolutional neural network segments yeast microscopy images with high accuracy. Nature Commun. **11**(1), 1–8 (2020)
12. Ferrari, A., Lombardi, S., Signoroni, A.: Bacterial colony counting by convolutional neural networks. In: Proceedings of EMBC 2015, pp. 7458–7461 (2015)
13. Hong, M., Yujie, W., Caihong, W., et al.: Study on heterotrophic bacteria colony counting based on image processing method. Control Instrum. Chem. Ind. **35**(3), 38–41 (2008)
14. Jiawei, Z., Chen, L., Rahaman, M., et al.: A comprehensive review of image analysis methods for microorganism counting: from classical image processing to deep learning approaches. Artif. Intell. Rev. **55**, 2875–2944 (2021)
15. Kingma, D., Ba, J.: Adam: a method for stochastic optimization. arXiv: 1412.6980 (2014)
16. Kosov, S., Shirahama, K., Li, C., et al.: Environmental microorganism classification using conditional random fields and deep convolutional neural networks. Pattern Recogn. **77**, 248–261 (2018)
17. Kulwa, F., Li, C., Zhao, X., et al.: A state-of-the-art survey for microorganism image segmentation methods and future potential. IEEE Access **7**, 100243–100269 (2019)
18. Kulwa, F., Li, C., Zhang, J., et al.: A new pairwise deep learning feature for environmental microorganism image analysis. Environmental Science and Pollution Research p, Online first (2022)
19. Li, C., Wang, K., Xu, N.: A survey for the applications of content-based microscopic image analysis in microorganism classification domains. Artif. Intell. Rev. **51**(4), 577–646 (2017). https://doi.org/10.1007/s10462-017-9572-4

20. Li, C., Zhang, J., Kulwa, F., Qi, S., Qi, Z.: A SARS-CoV-2 microscopic image dataset with ground truth images and visual features. In: Peng, Y., et al. (eds.) PRCV 2020. LNCS, vol. 12305, pp. 244–255. Springer, Cham (2020). https://doi.org/10.1007/978-3-030-60633-6_20
21. Oktay, O., Schlemper, J.F., et al.: Attention u-net: Learning where to look for the pancreas. arXiv: 1804.03999 (2018)
22. Rahaman, M., Li, C., Yao, Y., et al.: Identification of COVID-19 samples from chest X-Ray images using deep learning: a comparison of transfer learning approaches. J. X-ray Sci. Technol. **28**(5), 821–839 (2020)
23. Ronneberger, O., Fischer, P., Brox, T.: U-net: Convolutional networks for biomedical image segmentation. In: Proceedings of ICMICCAI 2015, pp. 234–241 (2015)
24. Selinummi, J., Seppälä, J., Yli-Harja, O., et al.: Software for quantification of labeled bacteria from digital microscope images by automated image analysis. Biotechniques **39**(6), 859–863 (2005)
25. Tang, Y., Ji, J.and Gao, S., et al.: A pruning neural network model in credit classification analysis. Comput. Intell. Neurosci. **2018**, 22 (2018). Article ID: 9390410
26. Xu, H., Li, C., Rahaman, M.M., et al.: An enhanced framework of generative adversarial networks (EF-GANs) for environmental microorganism image augmentation with limited rotation-invariant training data. IEEE Access **8**(1), 187455–187469 (2020)
27. Yamaguchi, N., Ichijo, T., Ogawa, M., et al.: Multicolor excitation direct counting of bacteria by fluorescence microscopy with the automated digital image analysis software BACS II. Bioimages **12**(1), 1–7 (2004)
28. Yoon, S., Lawrence, K., Park, B.: Automatic counting and classification of bacterial colonies using hyperspectral imaging. Food Bioprocess Technol. **8**(10), 2047–2065 (2015)
29. Yoshizawa, K.: Treatment of waste-water discharged from sake brewery using yeast. J. Ferment Technol. **56**, 389–395 (1978)
30. You, L., Zhao, D., Zhou, R., et al.: Distribution and function of dominant yeast species in the fermentation of strong-flavor baijiu. World J. Microbiol. Biotechnol. **37**(2), 1–12 (2021)
31. Zeiler, M., Krishnan, D., Taylor, G., et al.: Deconvolutional networks. In: Proceedings of of CVPR 2020, pp. 2528–2535 (2010)
32. Zeiler, M., Taylor, G., Fergus, R.: Adaptive deconvolutional networks for mid and high level feature learning. In: Proceedings of ICCV 2011, pp. 2018–2025 (2011)
33. Zhang, C., Chen, W., Liu, W., et al.: An automated bacterial colony counting system. In: Proceedings of SUTC 2008, pp. 233–240 (2008)
34. Zhang, H., Jian, L.: Current microbial techniques for biodegradation of wastewater with high lipid concentrations. Tech. Equipment Environ. Pollut. Control **3**, 28–32 (2004)
35. Zhang, J., Li, C., Kosov, S., et al.: LCU-net: a novel low-cost U-net for environmental microorganism image segmentation. Pattern Recogn. **115**, 107885 (2021)
36. Zhang, J., Li, C., Kulwa, F., et al.: A multi-scale CNN-CRF framework for environmental microorganism image segmentation. BioMed Res. Int. **2020**, 1–27 (2020)
37. Zhang, R., Zhao, S., Jin, Z., et al.: Application of SVM in the food bacteria image recognition and count. In: Proceedings of ICISP 2010, vol. 4, pp. 1819–1823 (2010)
38. Zhao, P., Li, C., Rahaman, M.M., et al.: Comparative study of deep learning classification methods on a small environmental microorganism image dataset (EMDS-6): from convolutional neural networks to visual transformers. Front. Microbiol. **13**, 792166 (2022). https://doi.org/10.3389/fmicb.2022.792166